THE DEVELOPMENT OF DESIGN CRITERIA FOR A ROTATING DISK CONTAINING NONCENTRAL CIRCULAR HOLE PATTERNS

by

WILLIAM BUCKNER HAILE, JR.

Thesis submitted to the Graduate Faculty of the
Virginia Polytechnic Institute
in candidacy for the degree of

MASTER OF SCIENCE

in

Engineering Mechanics

May 31, 1965

Blacksburg, Virginia

II TABLE OF CONTENTS

Section		Page
I.	Title	1
II.	Table of Contents	2
III.	List of Figures	3
IV.	List of Symbols	4
V.	Introduction	6
VI.	Review of the Literature	8
VII.	The Investigation	12
	A. Mathematical Approximation	13
	B. Experimental Methods	30
VIII.	Results	43
IX.	Conclusions	47
X.	Bibliography	49
XI.	Vita	52
XII.	Appendix A	54
XIII.	Appendix B	61

III LIST OF FIGURES

Figure 1	The Problem Investigated by C. B. Ling
Figure 2	Ling's Solution in Tabular Form
Figure 3a and 3b	Ling's Solution in Graphical Form
Figure 4	A Single Hole in a Uniform Stress Field
Figure 5	A Single Hole in a Uniformly Varying Stress Field
Figure 6	The Stresses in a Spinning Disk
Figure 7	The Disk with Noncentral Circular Holes
Figure 8	Material Properties at Room Temperature
Figure 9	Test Assembly
Figure 10	Test Disk and Fringe Patterns
Figure 11	Comparison of Experimental and Theoretical Results
Figure 12	Stress Concentrations for a Hole Near a Boundary

IV LIST OF SYMBOLS

A	The value of bipolar coordinate E at the edge of a hole. See appendix.
B, E	Bipolar coordinates. See appendix.
b	Radius of the noncentral holes.
f	Material fringe value
K	A parametric coefficient
K_{LO}, K_{LA}	Stress concentration factor due to longitudinal or lateral loading in Ling's solution.
L	The number of diameters center to center of adjacent holes measured along the circular arc between them.
M	Slope of the tangential stress field in a solid disk.
n	A positive integer, 0, 1, 2, ... either used in a series or used to indicate the number of holes.
R	Radius to the center line of the holes.
R_i	Radius of the central hole of the disk.
R_o	Radius of the outside edge of the disk.
S	Normal stress.
S_1, S_2	Stress at point 1 or 2 on a noncentral hole.
S_{BB}	Stress at the edge of a hole from Ling's solution. See appendix.
S_H	Horizontal stress.
S_R	Radial stress in a solid disk at radius R.
S_T	Tangential stress in a solid disk at radius R.
T	Uniform stress on the edge of a plate containing two holes.
t	Thickness of the disk.

θ Angle measured at the center of a hole from a tangential direction to an outward radial direction.

υ Poisson's ratio.

ρ Density of the disk.

ω Angular velocity of the disk.

V INTRODUCTION

In any flywheel, rotor, or disk shaped machine element a particular stress pattern is developed when the part is rotated about its center. The pattern is especially interesting if the disk contains a cut-out in its interior surface. For the case of a single circular central hole, the solution to the stress state is readily obtainable from Timoshenko and Goodier (reference 1). If the hole is away from the center, finding the stresses becomes a difficult task. Such a problem has been studied mathematically by Udoguchi (reference 2) and Newton (reference 4) and experimentally by Barnhart, Hale, and Meriam (reference 3), Newton (reference 4), Edmunds (reference 5), Ku (reference 6), and Ito (reference 23) so that some information is available on this topic. Consider now a ring of noncentral circular holes symmetrically placed about the center of the disk. A theoretical solution in closed form has not been obtained to this problem, and for noncentral holes, a formulation of the elasticity problem would indicate that such a solution would be complex. Therefore, a simplified approximate method of analysis is developed and the results verified experimentally. The difference in values of stress concentration factors obtained experimentally and by the approximate method are within 10% of one another.

The author wishes to express his appreciation to Professor Charles William Smith for his assistance and objective criticism in

obtaining and evaluating the resulting work. Many areas would be lacking in depth and completeness without Professor Smith's suggestions. A word of thanks is also extended to George Kenneth McCauley, Laboratory Instructor in Engineering Mechanics, for his much needed help in conducting experiments.

VI REVIEW OF THE LITERATURE

A review of the literature revealed a number of papers on the general subject of stress in rotating disks with non-central holes. From these, a brief sketch of the major sources of information is presented.

The most complete investigation of the subject is presented by K. E. Barnhart, A. L. Hale, and J. L. Meriam in their article,"Stresses in Rotating Disks Due to Noncentral Holes", (reference 3). The authors conducted a number of experiments with rotating disks and evaluated the results using methods of photoelasticity. Several different circular configurations were cut in the disk and studied. Models were cut from Fosterite and subjected to a "stress freezing" technique to obtain the stress pattern. The stress freezing method consists of placing a loaded model in an oven, heating the model (to about 120° F in this case), loading it in the desired manner, then slowly cooling the model to room temperature. If the process is performed well, the stress state of the loaded, and heated, model will remain when the model is cooled and the load removed. Stress patterns may then be examined at leisure in a polariscope. The reference presents a detailed method of stress freezing and the equipment necessary to perform the operation. The authors then investigated the case of a single noncentral hole in a spinning disk by varying hole size and radial location. Extensive graphs

are used to present the information obtained. Further studies were conducted on disks which had a central hole and six or ten noncentral holes equally spaced and of equal size. Again the results are given in graphical form using a stress concentration factor at the points of highest stress. A theoretical approximation is developed and compared to the experimental results. The approximation utilizes results from the state of stress about a single hole in an infinite plate loaded biaxially. The resulting equation is simple and easily applied, but tends to differ from laboratory tests at the points of maximum stress.

Additional tests were reported by H. G. Edmunds in his article, "Stress Concentrations at Holes in Rotating Discs" (reference 5). A disk with four noncentral and one central hole was spun in a polariscope and data collected by photoelastic methods. Models were cut from Catalin 800. Edmunds work was done in an attempt to verify a much simplified theoretical solution proposed by Teverosky, (reference 7). A few results were reported, but the data lacks the completeness necessary to be conclusive.

In the article by Green, Hooper, and Hetherington (reference 18) a solution is given for several disks with noncentral circular holes. Results are obtained for particular disks using an electronic computer and the Liebman iteration method to solve the governing differential equation. No closed form of solution is given. Bosses around the noncentral holes are studied as well as disks of tapering thickness. The authors found good agreement with experimental work done by Leist and Weber (reference 21). The tapered disk had no significant effect

on the stresses around the noncentral holes. Adding bosses at the holes had little effect on the hoop stress but greatly reduced the radial stress componet at the holes. The maximum stress concentration factor was essentially unchanged.

M. Hetenyi (reference 14), ran a series of experiments with a rotating disk of Bakelite 61-893. The model contained one central and two opposite noncentral holes. By measuring the change in the thickness of the disk before and after loading, stresses were computed. Hetenyi's data was later compared to the solution proposed by Barnhart, Hale, and Meriam (reference 3) by Ta-Cheng Ku (reference 6). Results, shown graphically, indicate fair agreement except at points distant from the noncentral holes.

For the method of analysis used to check results in this thesis, work done by E. K. Lynn (reference 8) proved to be quite useful. Lynn investigated a disk shaped pump rotor having various cut-outs using photoelastic methods. Data were obtained by taking high speed pictures of the model rotating in a polariscope with a stroboscopic flash. A flash duration of 0.00007 seconds gave good clarity to the photographs, but the type of film used was not stated. Columbia Resin 39 (CR-39) was used for the model material.

Numerous sources of information were investigated before beginning the formulation of a mathematical solution to the problem. It was hoped that work done previously might be expanded to include

noncentral holes in a spinning disk. Udoguchi (reference 2) examined the case of a single noncentral hole. His work was thorough and complete. However, the results were, necessarily, of such a complex nature that easy-to-use values could not be obtained. P. P. Radkowski (reference 9) explored the stress in a disk containing a number of noncentral holes. However, Radkowski did not spin the disk but loaded it on its outer border. For this reason, his results could not be applied to this paper. R. C. J. Howland (reference 10) conducted an investigation of the effect of neighboring holes on the one being studied. Howland's results were of a completely general form but not readily adaptable to design procedures. K. J. Schulz (reference 11) proceeded along the same lines as Howland but extended the work somewhat further.

In the paper "On the Stress in a Plate Containing Two Circular Holes", by C. B. Ling (reference 12), a result was found which was adaptable to the spinning disk problem. Ling studied two holes in an infinite plate loaded uniformly either transversely or laterally using the methods of elasticity in bipolar coordinates. A brief outline of Ling's work is presented in the appendix. By suitably combining Ling's solution with that of Timoshenko and Goodier (reference 1), the final form of the stress state in the neighborhood of the noncentral holes was developed.

Other references are discussed where appropriate in the following pages.

VII THE INVESTIGATION

When the problem of a spinning disk containing several eccentric circular holes is considered, it is immediately evident that a great number of variables is involved. Therefore, a complete mathematical treatment would necessarily be complex and clumsy to use. To simplify matters, an approximate investigation is formulated which yields good results that are easy to apply. To verify the accuracy of this work, several tests were conducted and experimental stress values compared to the theoretical ones. Findings indicate that the approximate theoretical treatment is close enough to the real condition to be significant. Though the results could be extended to include the entire disk, the final expression has been reduced to application only at the point of maximum stress concentration at the non-central holes, since this is of primary concern to the designer.

A Mathematical Approximation

By correctly combining solutions to similar problems, it is possible to approximate the true stress state in the disk. Furthermore, since only the points of maximum stress are usually desired, an approximation need not apply throughout the body, but only at specified points. The formulation is for holes distant from a boundary and not exceedingly close together, though allowances are made later if these conditions are not met. With this in mind, the following approach is presented.

Chih-Bing Ling (reference 6) has solved the elasticity problem of two nearby holes in an infinite plate uniformly loaded either laterally or longitudinally. A sketch of his work is included in appendix A. Using Ling's results, the stress at the edge of the hole is

$$\frac{S_{BB}}{T} = 2(\cosh A - \cos B)\left[K \sinh A\left(1 + 4\sum_{n=1}^{\infty} \frac{\sinh A \cos B}{\sinh 2nA + n \sinh 2A}\right)\right. \tag{1}$$

$$\left. \mp 2\sum_{n=1}^{\infty} \frac{n \cos nB\,(n \sinh nA \sinh A - \cosh nA \cosh A)}{\sinh 2nA + n \sinh 2A}\right].$$

K is a parametric coefficient and is found from

$$K\left[\frac{1}{2} + \tanh A \sinh A - 4\sum_{n=2}^{\infty} \frac{e^{-nA}\sinh nA + n \sinh A\,(n \sinh A + \cosh A)}{n(n^2-1)(\sinh 2nA + n \sinh 2A)}\right]$$

$$= \frac{1}{2} \pm \frac{1}{2} \mp 2 \sinh^2 A \sum_{n=1}^{\infty} \frac{n}{\sinh 2nA + n \sinh 2A} \cdot \qquad (2)$$

A and B are obtained from the relations

$$\cosh A = L \text{ , and } \quad \cos B = \frac{1 + L \cos\theta}{L + \cos\theta} \cdot \qquad (3)$$

In these equations where an ambiguous sign exists, the top sign is for a plate loaded in uniform longitudinal tension, and the bottom sign is for the plate loaded in uniform lateral tension. S_{BB} represents the stress at the edge of a hole and T is the magnitude of the uniform tension. The radius of a hole is b. L is given in terms of the distance between centers of the holes which is 2Lb. Figure (1) shows the plate and describes the symbols noted above.

The points of maximum stress are of most concern. They are labeled 1 and 2 in figure (1) where $\theta = \pm 90^{\circ}$. Actually, when the holes are close to one another or L is small, the points of maximum stress shift slightly to $85^{\circ} < \theta < 90^{\circ}$. However, if it is assumed that the maximum stress occurs at $\theta = \pm 90^{\circ}$ there will be little error.

The solution to equations (1), (2), and (3) is time consuming and there is a chance of computational error. To assist the reader, the equations were programmed in Fortran on an IBM 1620 computer and

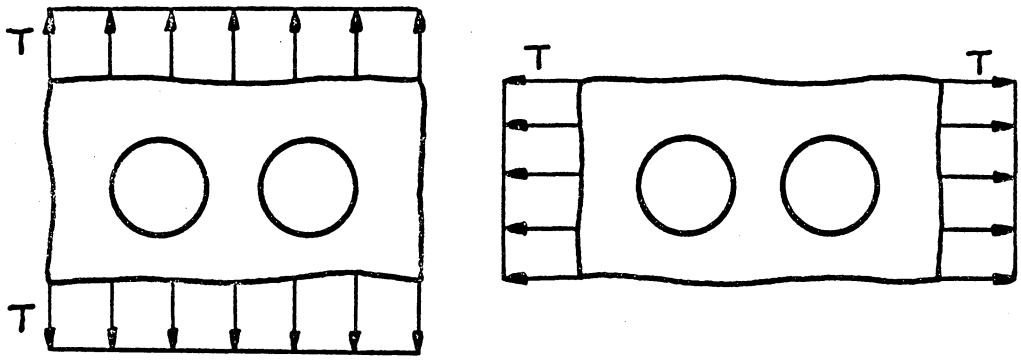

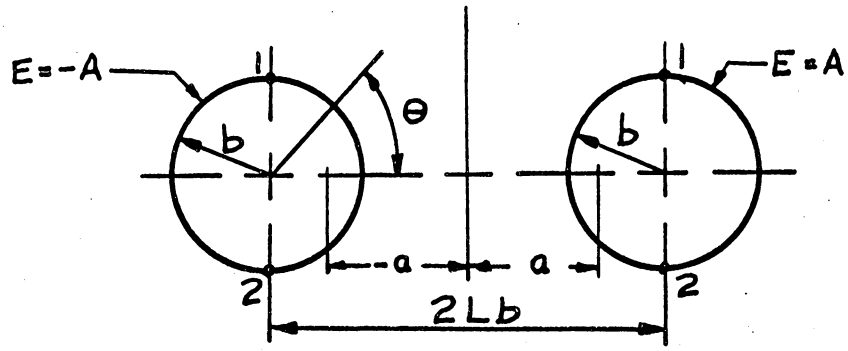

THE PROBLEM INVESTIGATED BY C. B. LING

FIGURE 1

solved for various values of L at $\theta=\pm 90^{\circ}$. Data obtained from the computer are displayed in tabular form in figure (2) and in graphical form in figures (3A) and (3B). For all later work, solutions to the previous equations are taken from the graphs. The results from the graph are in the form of a stress concentration factor. This is done by setting T equal to unity and K_{LO} and K_{LA} the stresses due to the longitudinal loading and lateral loading respectively.

Next consider the case of a single circular hole in an infinite plate under the action of a uniform simple tension. See the top of figure (4). From reference 2, the stress at the edge of the hole will be

$$S_r = S_{r\theta} = 0 \ , \quad S_\theta = S - 2S \cos 2\theta. \tag{4}$$

Rotating the figure 90° and adding this solution to the previous one, the plate loaded in two perpendicular directions pictured in the bottom of figure (4) is described. Here the stress at the edge of the hole is

$$S_\theta = S_H + S_V - 2(S_H - S_V)\cos 2\theta \tag{5}$$

where S_H is the larger of the two edge loadings. At points 1 and 2 where $\theta = 90^{0}$

$$S_\theta = 3S_H - S_V \, . \tag{6}$$

Now consider the case of a single circular hole in an infinite plate under a uniform bending at infinity. The top of figure (5) shows this condition. In the figure, M represents the slope of the uniformly varying stress. From reference 7, the stress at the edge of the hole

STRESS CONCENTRATION FACTOR AT $\theta = 90^{\circ}$

SOLUTION TO LINGS EQUATION

L	LONGITUDINAL LOAD	LATERAL LOAD
10.000	2.98027	-.99012
6.500	2.95495	-.97780
5.000	2.92668	-.96438
4.500	2.91130	-.95722
3.800	2.88084	-.94342
3.200	2.84183	-.92662
2.700	2.79549	-.90836
2.300	2.74653	-.89195
2.000	2.70262	-.88124
1.800	2.67094	-.87748
1.600	2.63883	-.87956
1.400	2.60789	-.89205
1.200	2.57974	-.92430
1.100	2.56824	-.95805
1.020	2.56379	-1.01968

LING'S SOLUTION IN TABULAR FORM

FIGURE 2

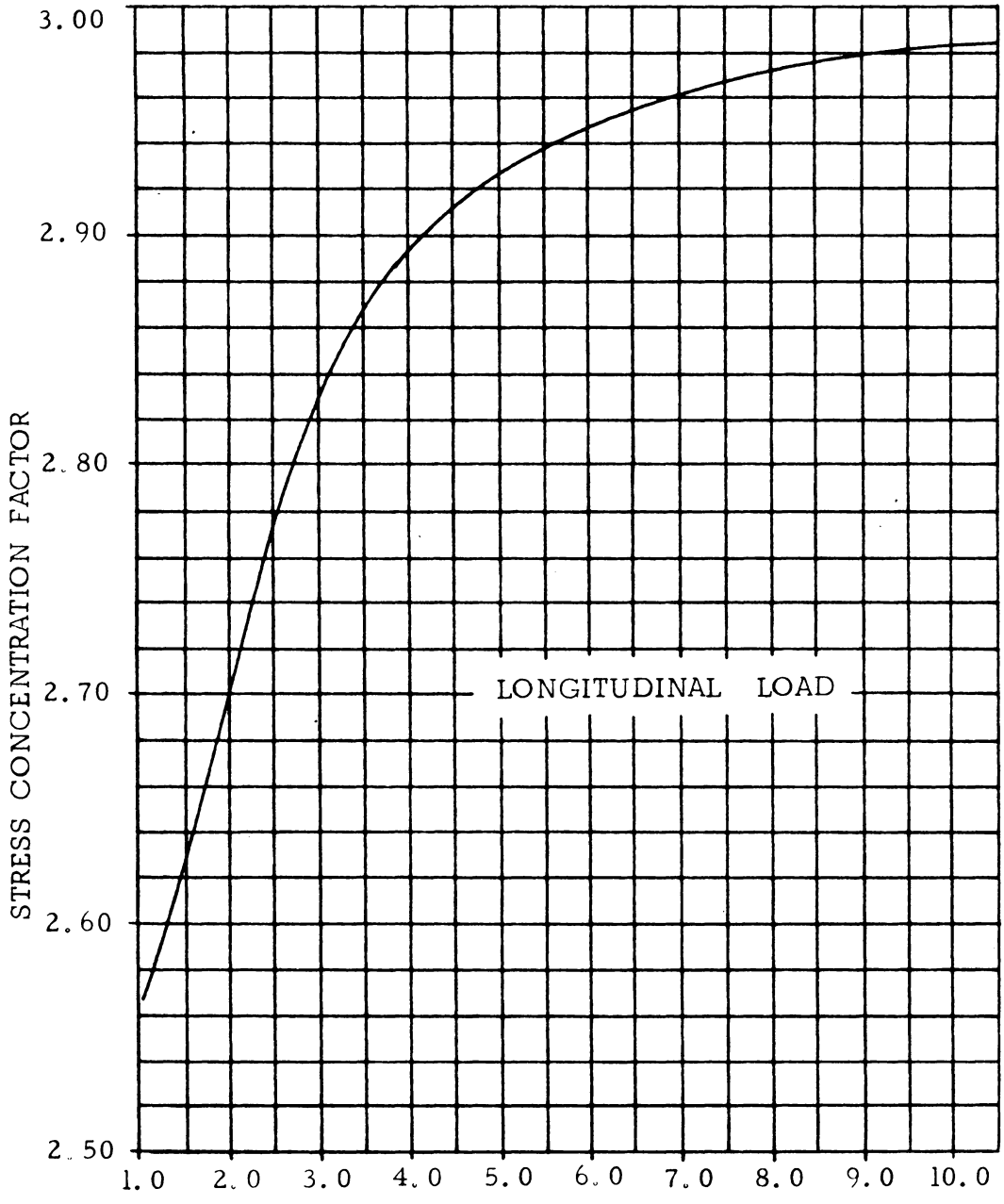

LING'S SOLUTION IN GRAPHICAL FORM

FIGURE 3A

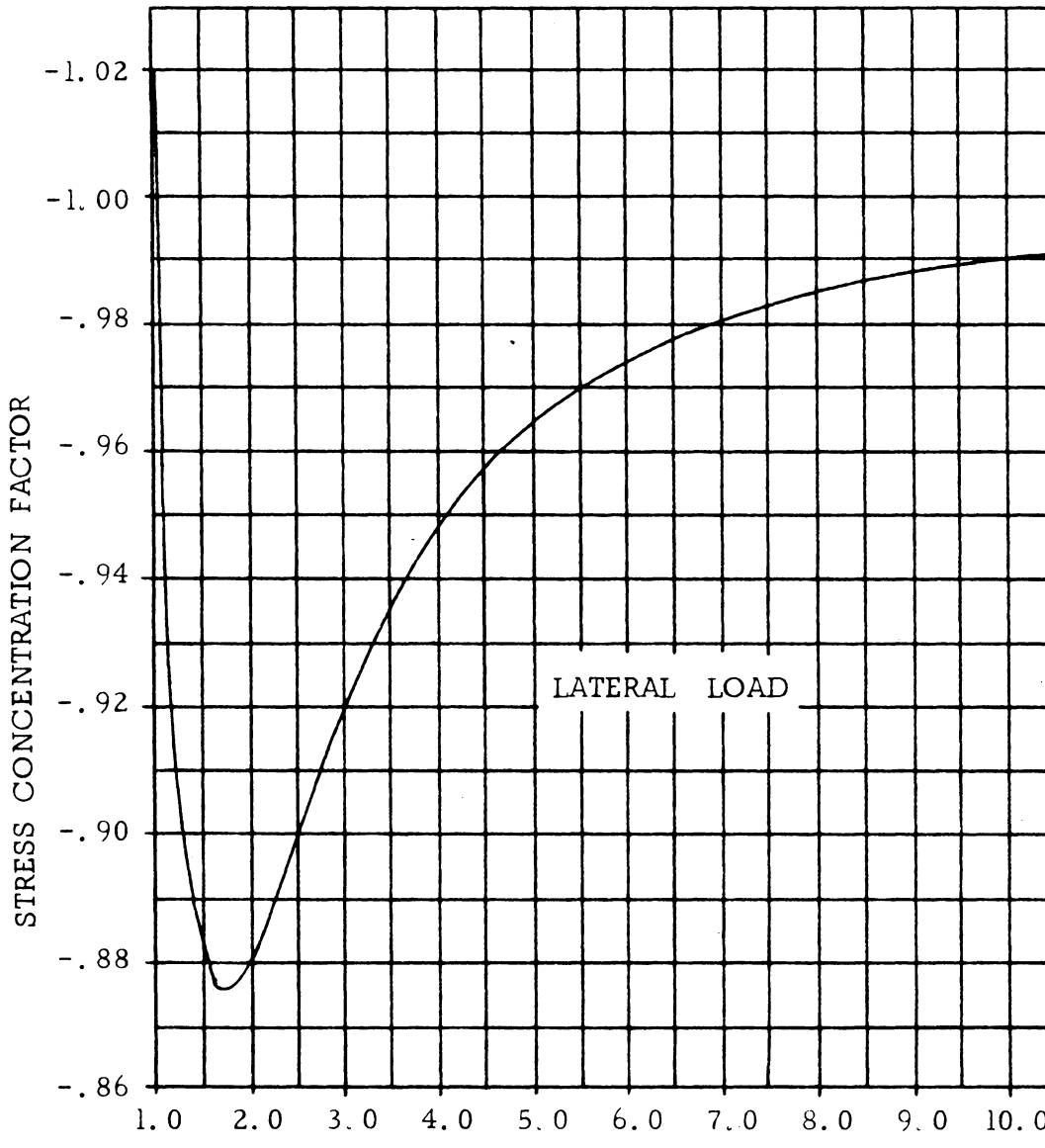

LING'S SOLUTION IN GRAPHICAL FORM

FIGURE 3B

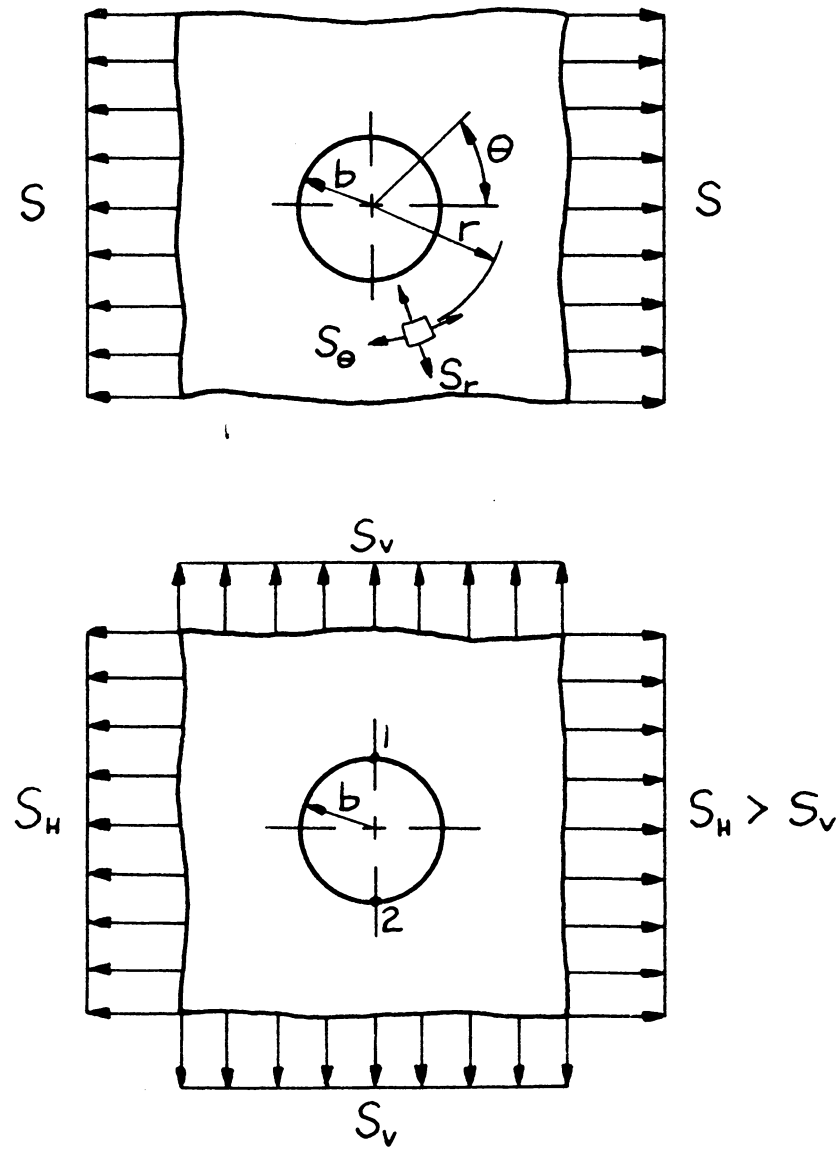

A SINGLE HOLE IN A UNIFORM

STRESS FIELD

FIGURE 4

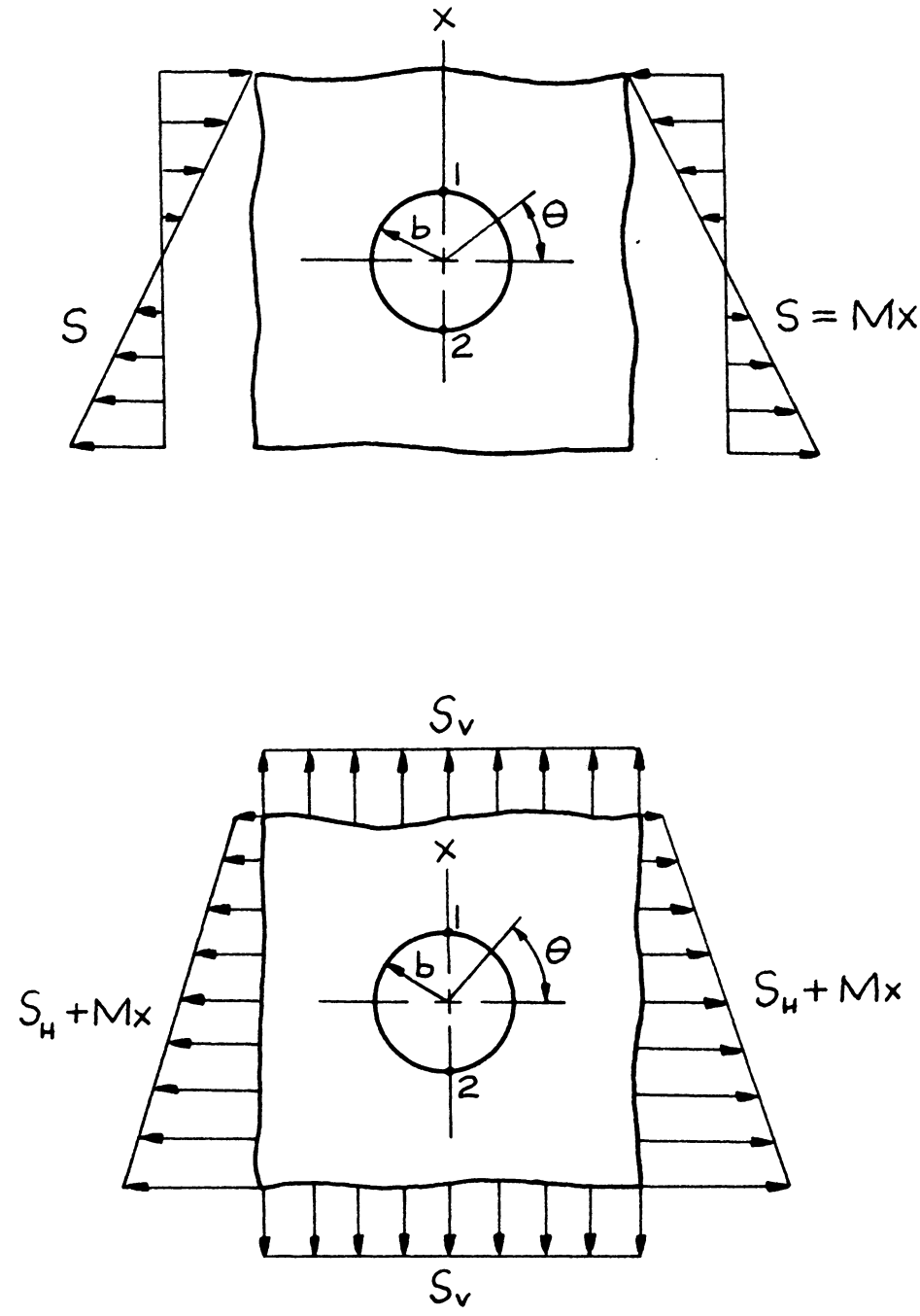

A SINGLE HOLE IN A UNIFORMLY VARYING STRESS FIELD

FIGURE 5

is

$$S_\theta = 2Mb \sin\theta \cos 2\theta. \tag{7}$$

At points 1 and 2, respectively

$$S_{1,2} = \mp 2Mb. \tag{8}$$

By combining equations (5) and (7), we arrive at the condition pictured in the lower portion of figure (5). Here the stresses at points 1 and 2 are

$$S_{1,2} = 3S_H - S_V \mp 2Mb. \tag{9}$$

Proceeding in this manner, using proper values for S_H, S_V, and M, and adding correct stress concentration factors, an approximate solution to the state of stress around the noncentral holes in a spinning disk may be derived.

We begin by first finding expressions for the values of the stresses and postpone the search for stress concentration factors for several paragraphs. Consider a solid circular disk of outer radius R_o which may have a central hole of radius R_i as shown at the top of figure 6. When rotated about its center with angular velocity ω, the stresses in the solid disk from reference 1 are

$$S_r = \frac{3+\nu}{8}\rho\omega^2\left(R_o^2 + R_i^2 - \frac{R_o^2 R_i^2}{r^2} - r^2\right) \tag{10}$$

$$S_\theta = \frac{3+\nu}{8}\rho\omega^2\left(R_o^2 + R_i^2 + \frac{R_o^2 R_i^2}{r^2} - \frac{1+3\nu}{3+\nu} r^2\right) \tag{11}$$

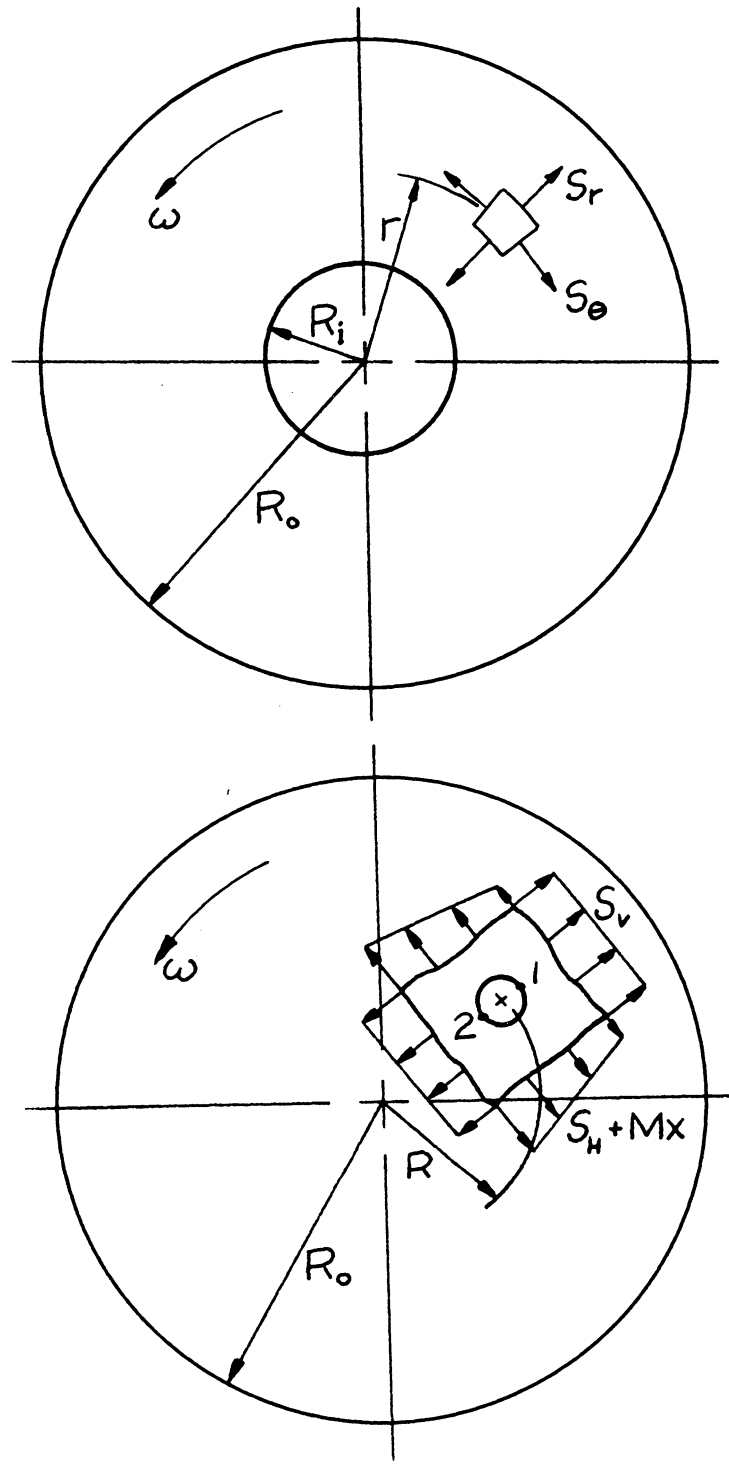

THE STRESSES IN A SPINNING DISK

FIGURE 6

where ν is Poisson's ratio and ρ is the density of the disk. Here the solution is for a disk with a central hole. If the disk contains no such hole then it is necessary only to set $R_i = 0$ in the above two equations.

Now, place a single eccentric hole in the disk at a radius R out from the center. Let the uniform stresses S_H and S_V be the values of the solid disk stresses S_r and S_θ and let M be the rate of change of the stress S_θ in the r direction. That is

$$\left.\begin{aligned} S_H &= S_\theta \\ S_V &= S_r \\ M &= \frac{dS_\theta}{dr} = -\frac{3+\nu}{4}\rho\omega^2\left(\frac{R_o^2 R_i^2}{r^3} + \frac{1+3\nu}{3+\nu}r\right). \end{aligned}\right\} \quad (12)$$

By setting $R_i = 0$ the condition pictured in the lower portion of figure (6) is obtained. At points 1 and 2, $r = R \pm b$ respectively.

It is desired next to consider a ring of identical holes placed at a constant radius out from the center of the disk. To extend the previous formulation to this case, approximate stress concentration factors must be employed. There will be a certain amount of interaction between the holes so that the stress fields of neighboring holes must be accounted for as well as the one under consideration. Here a simplified technique is employed. It is assumed that only adjacent holes effect the stress at the one being studied so that holes farther away than this may be ignored. Or, the assumption is

made that the disk contains only three noncentral holes, side by side, and the one in the middle is to be studied.

From equation (9) the concentration factor due to S_H on one hole is 3. To include a single neighbor, the results of equation (1) shown in figure (3A) should be employed so that the stress concentration factor becomes K_{LO}. K_{LO} is less than three so the effect of a second hole is to decrease the stress on the first. In another way, this may be obtained by taking the concentration factor due to one hole, 3, and multiply it by $K_{LO}/3$, a number less than unity to account for the second hole. For three holes, the stress on the middle one should be reduced further below K_{LO} or below $(K_{LO}/3)$. A convenient method would be to multiply by $K_{LO}/3$ again to include effects due to the third hole. Then the stress concentration factor becomes $(K_{LO}/3)\ 3\ (K_{LO}/3)$. Similarly, the appropriate stress concentration factor to place before S_V is $-(K_{LA}/1)\ 1\ (K_{LA}/1)$ and not -1 as appears in equation (6).

Further investigation of equations (6) and (8) reveals that stresses due to the linearly varying normal load are only 2/3 as great as from simple tension. Since this varying load is in the same direction as S_H, let its coefficient for three holes be $2/3\ (K_{LO}^2/3)$.

Combing what has just been stated, it appears as though the form of the maximum stresses about the noncentral holes from the superimposed solutions should be

$$S_{1,2} = \frac{K_{LO}^2}{3}\left(S_H \pm \frac{2}{3}Mb\right) - K_{LA}^2 S_V \cdot \qquad (13)$$

Where the ambiguous sign appears, the top sign is for point 1 and the bottom sign is for point 2. There is, however, still more to be said before the final form of the equation is presented.

In equation (13), the values of S_H, S_V, and M are calculated at the center of the noncentral hole, at r=R. If the holes are large or in a region of high stress gradient, this may lead to inaccuracies. In an effort to overcome this difficulty, we begin by letting S_H be calculated at either point 1 or point 2 (at $r=R\pm b$) in equation (13). Furthermore, let the uniformly varying load, M. also be found at points 1 or 2. The coefficient 2/3 is now no longer appropriate. Instead of adding 2/3 of the effect of M, subtract 1/3 of its effect when it is calculated at the points being studied. An in-between value is needed for S_V as it is felt by the entire hole and not just at a particular point. Let it remain as before and be calculated at r=R, the center of the noncentral hole. Therefore, the final form of the equation for the stresses at points 1 and 2, the points of maximum stress, should read

$$S_{1,2} = \frac{K_{LO}^2}{3}\left(S_H \mp \frac{1}{3}Mb\right) - K_{LA}^2 S_V \qquad (14)$$

where

$$S_H = S_\theta \quad at \quad r = R \pm b$$

$$S_V = S_r \quad at \quad r = R$$

$$M = \frac{dS_\theta}{dr} \quad at \quad r = R \pm b.$$

S_θ and S_r are found from equations (10) and (11) and M from equation (12). Plugging in values of S_H, S_V, and M and simplifying results, equation (14) is rewritten as

$$S_{1,2} = \frac{3+\nu}{8}\rho\omega^2\left[(R_o^2+R_i^2)\left(\frac{K_{LO}^2}{3}-K_{LA}^2\right)+\frac{K_{LO}^2}{3}\frac{R_o^2R_i^2}{r^2}\left(1\pm\frac{2b}{3r}\right)\right.$$
$$\left.-\frac{K_{LO}^2}{3}\frac{1+3\nu}{3+\nu}r^2\left(1\mp\frac{2b}{3r}\right)-K_{LA}^2\left(\frac{R_o^2R_i^2}{R^2}+R^2\right)\right] \qquad (15)$$

where $r=R\pm b$ at points 1 and 2. K_{LO} and K_{LA} are formed from figures (3A) and (3B) and the value L is found shown in figure (1). L is now the number of diameters center to center of two adjacent holes measured along the circular arc between them. Its value is

$$L = \frac{\pi R}{n b} \qquad (16)$$

where n is the total number of noncentral holes. Figure 7 shows a typical disk to which this result may be applied.

Two comments are necessary before applying the final equation (15). First, after checking calculated values against experimental results which follow and results from reference (3), it was noticed

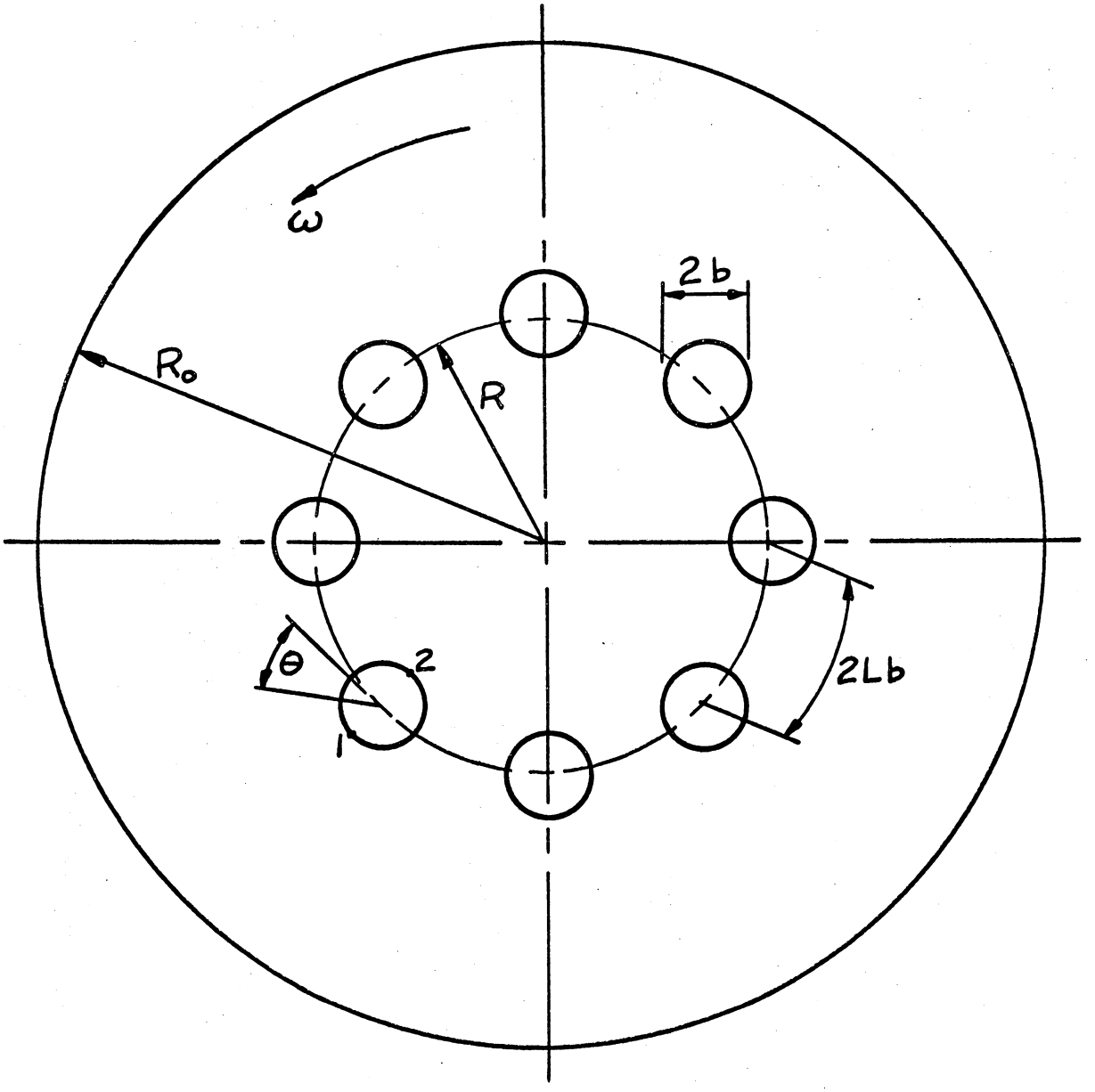

THE DISK WITH NONCENTRAL CIRCULAR HOLES

FIGURE 7

that equation (15) yielded good results for point 2 but was consistently off for point 1. In order to arrive at better agreement with observations, for point 1 only, replace $K_{LO}^2/3$ with K_{LO} and K_{LA}^2 with K_{LA} and calculations should be within 10% accuracy. This adjustment is equivalent to saying that for point 1, the outside point, there is only one neighboring hole and not two as previously assumed. The reason for this modification can not be given. The second comment is that when the noncentral holes are close (within two diameters) to a solid boundary, an additional concentration becomes significant. The amount of change in the stress due to a boundary is sometimes quite important and, for this reason, appendix B is included which gives a graphical result from reference (15). To include this effect, multiply the stress found from equation (15) by the stress concentration factor indicated in appendix B.

The disk with its holes is a multiply connected body so there may be some question as to the validity of superimposing solutions in this case. Perhaps an adjustment of Poisson's ratio is necessary. However, when Poisson's ratio was varied from 0.2 to 0.5 in equation (15) the value of stress obtained differed by only 2%. This is not considered to have enough significance to include when one considers experimental error and the approximations already imposed.

B Experimental Methods

The most direct method of finding stresses in an irregularly shaped body is to build one and test it in the laboratory. Partly for this reason and partly to check the mathematical theory, a disk was designed and investigated using photoelastic techniques.

The problem, being one of plane stress, lends itself well to study by photoelastic methods. If a model could be photographed accurately when under the dynamic load experienced by a spinning disk, good results should be obtainable. Available literature on testing procedures deals primarily with the "stress freezing" methods. As the equipment necessary for the these tests was not available, a different approach would have to be pursued here. It was decided to rotate the disks in a polariscope and photograph results using a high speed strobe flash unit to "stop" the action. This required a particular mount which would hold the model securely yet allow light to pass through it in the region of investigation. Many difficulties had to be overcome and several variations of the proposed laboratory method were tried before any results were obtained.

It is assumed that the reader is familiar with the operation of a polariscope and the techniques of photoelasticity. If not, refer to Frocht, reference 16.

To achieve a high stress condition in the disk which would

yield many photoelastic fringes when viewed in a polariscope, it is necessary to spin the disk at a high angular velocity. Due to instrumental limitations and sizes of available photoelastic materials, a disk of about eleven inch diameter was chosen as being the largest that could satisfactorily be used. Depending on the model material chosen and its material fringe value, such a size indicates that disk speeds on the order of 6,000 to 12,000 rpm are necessary for good results. Such speeds are excessive and should be attempted only with sturdy, carefully assembled equipment machined to close tolerances. As most of the parts used in the laboratory had to be hand built by the experimenter, it was decided not to attempt such high speeds for reasons of safety. It was hoped that tests could be conducted at speeds less than 3,000 rpm. A model 1/4 inches thick with a material fringe value of 4 or 5 would be adequate for the proposed tests; but no material was located which would exhibit this fringe value at ordinary temperatures.

Two relatively recently developed materials were found which have been used in high temperature photoelastic work. Several previous experimenters had used other materials in the stress freezing technique and reported good results (references 3,4,5). It appeared that by heating the model, the fringe value decreased until enough fringes appeared in the model to give accurate readings. The stress freezing method was discarded as the experimental procedure to follow in this thesis as it requires carefully balanced parts and a well regulated

oven whicn will allow a temperature drop of some 10 degrees F per hour. The system is quite sensitive to any rapid thermal changes or load variations. Such equipment was not available. However, it was thought that if a crude oven could be procured which would maintain a constant temperature, perhaps the models could be photographed while hot. This idea was pursued to its conclusion.

An oven was designed and built to fit in the polariscope. The most important features were two 1,000 watt strip heaters located in the base, one half inch of asbestos insulation secured to galvanized steel plate walls, a plus or minus one degree F thermocouple to maintain temperature, and two large 1/4 inch thick glass parts fore and aft allowing light to pass through the oven. Two thermometers were mounted to protrude out of the oven and were noticed to give consistently identical readings. An external motor fanned the air inside the oven to distribute the heated air uniformly. The usual static loading rig as well as the mount for the disk could fit easily inside of the oven space. Having assembled the oven the work proceeded to calibrate several materials at elevated temperatures.

The Hysol Corporation, Olean, New York, supplies CP 5 - 4290 which has a material fringe value of 28.5 at 77 degrees F but drops to 0.67 at 270 degrees F (see reference 19). This appeared to be a suitable material for the disk. Previous high temperature work on this Hysol product is sketchy, so calibration work had to begin from scratch. Bending and tensile models were cut and tested to find the fringe value

and to get an estimate of the creep rate at various temperatures. The fringe value remained essentially constant to 180 degrees F dropping only slightly. Between 180 and 220 degrees the fringe value decreased rapidly until at 230 degrees it was too low to measure accurately. Creep followed a similar pattern, remaining negligible until about 200 degrees. At 235 degrees a two inch length under 80 psi tension crept about 0.055 inches in two minutes which is too rapid to be considered for the dynamic loading of a spinning disk. The creep data must be considered only approximate as elongations were found by sighting through a theodolite at marks etched on the specimen. Accuracy is estimated at ±0.005 inches. At 230 degrees and higher the Hysol became quite flexible having roughly the same characteristics as rubber, and though the manufacturer lists a maximum tensile strength of 210 psi at 270 degrees F, nothing is said about creep rupture data. An additional property became apparent at high temperatures and should be commented upon. After three fringes are obtained in the model, any additional loading produced very fuzzy fringes which tended to lose clarity until after about six fringes they disappeared entirely. A similar result is reported by San Miguel and Duran, reference 22, in which they recommend that one should not exceed four fringes. Perhaps this is due to its relaxation or creep as the fringes begin interfering with one another through the thickness (1/4 inch) of the model. From San Miguel and Duran, this "wash out" may also be due to a chemical change which begins

at elevated temperatures. It was concluded that while the Hysol CP 5-4290 may be suitable for bulk stress freezing experiments where good local resistance is available it was of doubtful value for the present case of interest.

Another material, Cadco Lexan Polycarbonate, available from the Cadillac Plastic and Chemical Company, Detroit, Michigan, was also tested at elevated temperatures (see reference 20). The polycarbonate has the low material fringe value of 16.7 at room temperature, but no high temperature data was available. Again bending and tensile samples were cut and tested. The fringe value decreases only slightly until about 260 degrees F, after which it begins to fall rapidly. Creep was small here where only 0.005 inches was experienced at 190 psi load in a two inch length at temperatures as high as 290 degrees. At 310 degrees the material suddenly loses all strength and fails by rapid flow under the loading apparatus, at a load of about 20 psi. Ito, reference 23, reports a rapid drop in the Rockwell hardness of polycarbonate resins at about 290 degrees F and substantiates the low creep rates. However, the only available oven precluded maintaining a steady temperature throughout at anything above 270 degrees. This was the range in which use of this polycarbonate was to be made, and since this was also the range of rapid change in material fringe value and strength, it was decided not to use high temperature techniques on the Hysol product.

It is interesting to note that of the references listed which

used the stress freezing method of experimentation, no mention is made of creep, either measuring for it or compensating for it after the dynamic loading tests.

After checking the literature on other photoelastic materials, Cadco Lexan Polycarbonate was chosen as the best material with which to conduct tests as it had the lowest material fringe value at room temperature. High temperature testing was undesirable since little benefit could be gained by it toward reducing the fringe value until temperatures became high enough to introduce troublesome side effects.

The properties of the two previously discussed materials are shown in figure 8.

To produce eight fringes around the noncentral holes in a model of 5.5 inch radius, speeds of some 7,000 rpm would be necessary using the polycarbonate. For accurate reading of results at least eight fringes should be seen. Originally, it was hoped to test models without a central hole at speeds of 2,000 rpm. The testing rig was designed for such a loading with safety. To compromise, the rig was altered for strength and several tests were run at about 4,600 rpm, allowing only five fringes. Photographs obtained could be read to plus or minus 1/2 a fringe or within 10%. For a static test, the Tardy compensation method may be employed for precise fringe reading. This involves rotating the polariscope analyzer until a whole fringe is placed at the desired point and using the amount of rotation necessary to do this out of 180 degrees to calculate the fraction of a fringe

	HYSOL CP5-4290	CADCO LEXAN POLYCARBONATE
Tensile yield strength, psi	12,000 210 at 270°F	8000-9000
Modulus of elasticity, psi	480,000 2190 at 270°F	340,000
Compressive strength, psi	18,000	11,000
Poisson's ratio	0.50	0.38
Specific gravity	1.20	1.20
Material fringe value*	28.5 20 at 190°F 0.67 at 270°F	16.7 13 at 250°F
Time edge effects	Slight	Slight

* Some values found experimentally

MATERIAL PROPERTIES AT ROOM TEMPERATURE

FIGURE 8

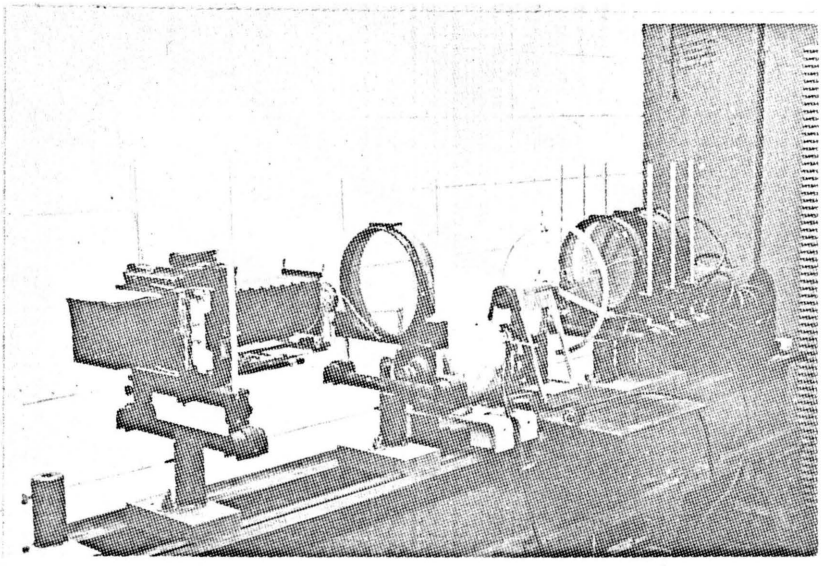

Testing Apparatus

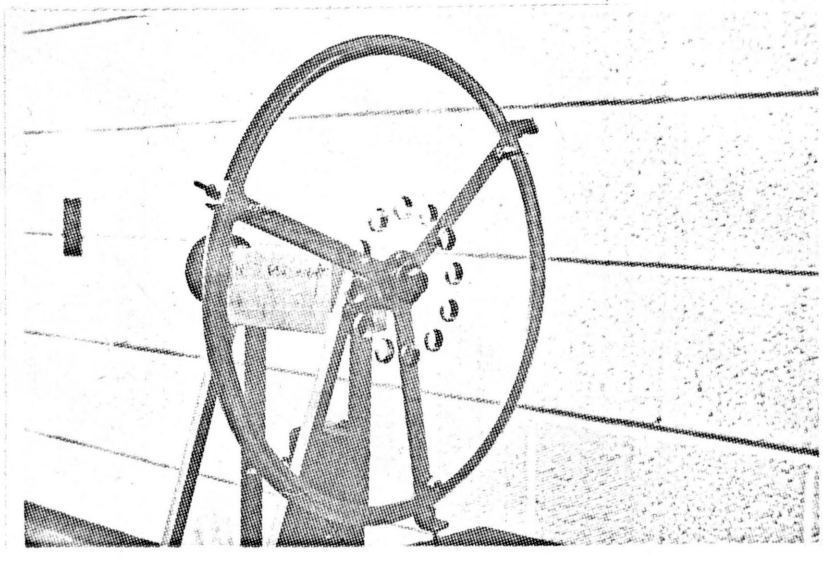

Disk and Mount

TEST ASSEMBLY

FIGURE 9

that actually exists at that point. On dynamic tests, this method is of course, impossible. The residual fringes around the holes before and after testing were found by the Tardy compensation method.

The disk mount was a three pronged aluminum wheel mounted at its center to an axle. A photograph is included in figure 9. At the outer edge, along the circular rim, were placed three SAE 4-40 size bolts which served a dual purpose. As a safety measure, they protruded inward to almost touch the disk's edge so that if the disk slipped slightly off-center, they would catch it and avoid an accident. Secondly, the mount was not dynamically balanced but only statically balanced. Due to circular symmetry this was thought to be sufficient. Small nuts could be placed on the bolts to improve the balance of the mount if it were necessary. After constuction, the balance of the system was checked and only one 4-40 nut was required on one of the bolts. On the outer ends of each of the three legs were placed SAE 10-32 size bolts which were used to attach the disk to the mount. They protruded some 1/2 inch out of the plane of the mount and allowed the disk to be bolted on loosely so that they would not restrain the straining of the disk when spun. The axle was held by two "1600" series, precision ground Nice ball bearings and driven by a 1/4 inch V-belt and pulleys. After several attempts to use 1/20 and 1/10 horsepower motors to provide the power, a 1/3 horsepower Powr-Kraft motor was selected. The smaller motors were unable to bring the disk up to the desired speed. The mount and assembly were raised in the polariscope by a rigid triangulated structure.

Test disks were cut from Cadco Lexan Polycarbonate plate, 1/4 inches thick. Several techniques were employed to obtain good, stress free models. First a 1/8 inch oversize disk was cut from the plate. An aluminum disk of the final desired size, 0.10 inches thick was glued to the rough cut-out to act as a template for the next operation. Using a high speed mill, the excess plastic was removed from the model slowly and evenly. A stop was provided to keep the template out of the mill. The flat surfaces of the model were checked for irregularities and did not need to be smoothed or polished. Since the disk was to run at a higher speed than originally planned, a central 3/8 hole was drilled in it into which the mounting axle was inserted. This was necessary as a safety measure to hold the disk in place. Admittedly, if the disk were out of balance, the central shaft would load the interior hole -- an undesirable effect. To minimize this effect, several photographs were taken of the spinning disk so that the fringes were counted at each noncentral hole and the average value taken. Three small holes were drilled near the outer periphery of the model and spaced every 120 degrees for attachment points to the mount. Each hole was elongated radially to allow for expansion of the model or the mount. These three points would fix the model yet provide no radial restraint. Lastly, the noncentral holes were drilled. A freshly sharpened undercut drill was used which removes material from the periphery first, then the center. This technique produces almost no residual stress at the holes. All plastics are sensitive to

thermal stresses, particularly photoelastic models. Great care must be taken when cutting these models, for residual stresses along the machined boundaries will mask stresses caused by laboratory loading. The most common cause of these undesirable edge effects is the temperature gradient produced by machining operations. The second most common cause is due to dull tools. In addition, the material may absorb moisture at a freshly cut surface and "time edge" effects begin to develop. In order to minimize these residual stresses, only freshly sharpened tools were used and all drilling was done under water. The noncentral holes were drilled only a few hours before the tests were conducted. Using the Tardy compensation method, completed models exhibited about 1/4 of a fringe at the noncentral hole boundaries. The sheet stock from which models were cut displayed 1/2 of a fringe uniformly throughout. This residual loading was retained in the completed disk. Models were not annealed as no facilities were available. However, since this residual load was uniform and retained at isotropic points which appeared under loading, fringes could be counted from the 1/2 of a fringe starting point.

To photograph the loaded model, a strobe flash unit was mounted in the polariscope in place of the usual light source. The model chosen was a Strobolume, Type No. 1532-A, from the General Radio Company. This item produces a brilliant flash of 30 to 40 microsecond duration. No attempt was made to trigger the flash for a particular disk position as photographs of several parts of the disk were desired

so results could be compared. For each test four photographs were taken which effectively covered all of the noncentral holes. The fringe pattern varied slightly between holes so an average value was taken as representative. Since the light must pass through a blue filter, the polarizer, analyzer, two quarter wave plates, and the loaded model, a high film speed was required. 3,000 Speed Polaroid Land 4x5 film Type 57 was used and produced satisfactory, high contrast prints at a camera setting of f.4. A sample is displayed in figure 10.

Tests were run with disks containing 6 and 12 noncentral holes. Counting the fringes at a hole was simplified because outward and midway between the holes was an isotropic point where the fringe order remains zero. Furthermore, since the stress was desired at a boundary, the fringe on the boundary represented half of the normal stress directly and not the usual maximum shearing stress. From the stress-optic law, the stress at a hole is then

$$\sigma = \frac{2nf}{t} \tag{17}$$

where n is the number of the fringe, f is the material fringe value, and t is the plate thickness. Results of the tests are discussed in the following section.

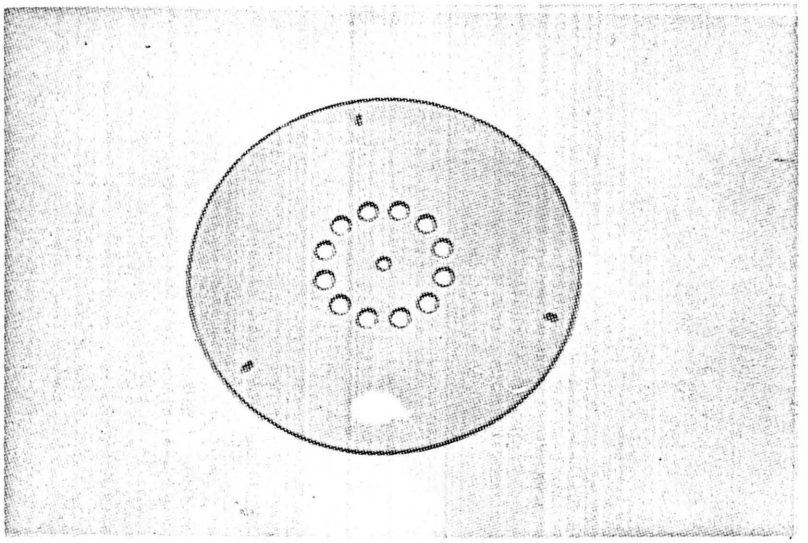

12 Hole Test Disk

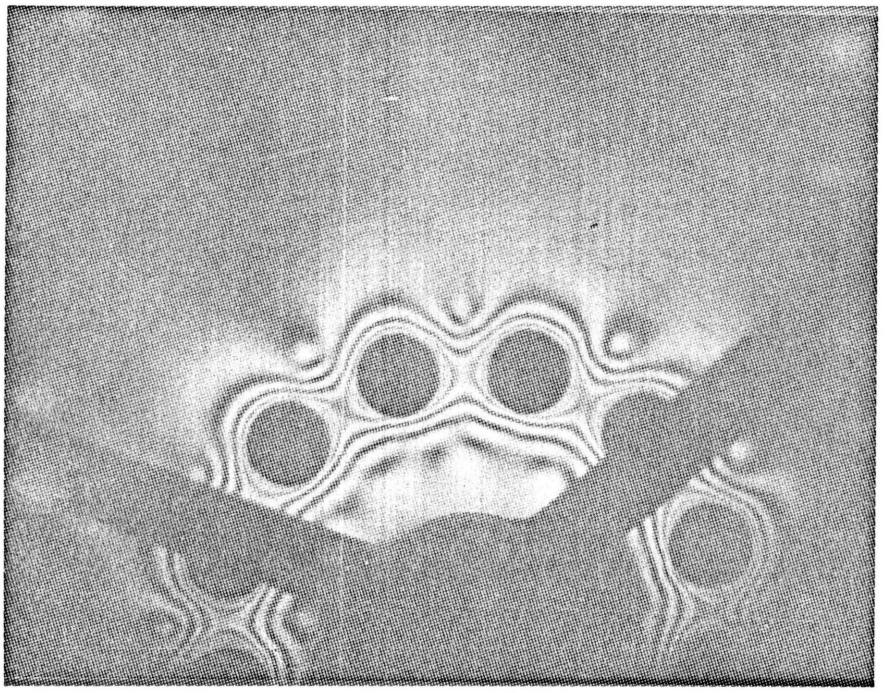

Results at 4590 RPM

TEST DISK AND FRINGE PATTERNS

FIGURE 10

VIII RESULTS.

The results of the work as completed will consist primarily of comparing the mathematical approximation with the experimental results.

The laboratory work previously described yielded results which were subject to some experimental error. Each disk had a shaft passing through its central hole. The force exerted by this shaft is difficult to measure and is not included in the mathematical theory. However, each test disk was checked for static balance before and after loading and displayed no out of balance behaviour. Also, the number of fringes around the holes differed little in the loaded model as willnot happen if there were a central load. Based on the above evidence, it is believed that the central shaft exerted little if any force on the disk.

As a material with the low fringe value desired was not discovered and the test apparatus was not built to withstand extremely high speeds, an intermediate speed had to be used for tests. This resulted in only above five fringes at the maximum in the six hole model and 4.5 fringes in the twelve hole model. Although the number of fringes and extent of interpolation used here will not yield the degree of accuracy normally desired in photoelastic research, it is felt that the data are within the limits of accuracy of the design criteria. All readings were taken to plus or minus 1/2 of a fringe A sample photograph of a loaded 12 hole disk is shown in figure 10.

Due to these difficulties, the experimental results were not

considered to be conclusive evidence of the verification of equation 15, even though agreement was within 5%. For additional experimental values, the most complete of the references was drawn upon as a further check of equation 15. The results found by Barnhard, Hale, and Meriam, reference 3, are shown in the following figure 11 along with those found experimentally. The stress concentration factor used is the stress found at points 1 or 2 divided by the stress that would exist at the same place in a solid disk without noncentral holes. It will be noticed that agreement is within 10%. Though the highest stress concentration appears at point 1, the greater stress is always at point 2, on the inside edge of the hole.

Experimental errors may be accounted for in the following way:

Specific gravity	1.20±0.01
Fringe value	16.7±0.2
Disk speed	4580±10 rpm
Disk dimensions	±0.02 in.
Disk thickness	0.247±0.001 in.
Number of fringes	±0.5

Using the tolerances above to give the maximum and minimum stresses, the $\rho\omega^2$ in the theoretical work is accurate to 2% as both ρ and ω are subject to some error. Proceeding in this way to give the maximum and minimum stresses and using the disk dimensions shown in figure 11, the results of the tests to two significant figures is as follows.

Maximum stress at hole boundaries in psi:

		Calculated	Experimental
6 Hole Disk	Pt. 1 (outside)	580 ± 3%	600 ± 12%
	Pt. 2 (inside)	560 ± 3%	580 ± 13%
12 Hole Disk	Pt. 1 (outside)	530 ± 3%	560 ± 14%
	Pt. 2 (inside)	470 ± 3%	430 ± 17%

The major reason for the inaccuracy in the experimental results is due to the reading of fringes.

Upon observing the sample photograph in figure 10 an interesting result is seen which was not accounted for in the theory. Ling's paper (reference 12) which was drawn upon previously does include this effect. Using it at these additional points would necessarily complicate the solution more than is felt desirable. When twelve large noncentral holes are placed in the disk, a shielding effect begins to appear and the largest stress is between the holes and not at their outer and inner extremities as predicted. The stress on inner boundary drops below the calculated value where as the stress at the outer boundary appears to remain uneffected. A similar result was noticed by Barnhart, Hale, and Meriam (reference 3) when they experimented with 10 hole disks. In their work, this effect was just beginning to appear. A continued treatment is contained in the conclusions which follow.

NO. OF HOLES	R_i	R	R_o	b	EXPERIMENTAL RESULTS		CALCULATED RESULTS	
					SCF_1	SCF_2	SCF_1	SCF_2
FROM TEST DISK								
6	.1875	1.7812	5.5625	.2812	1.96	1.76	1.88	1.73
12	"	"	"	"	1.73	1.23	1.63	1.37
FROM REFERENCE 3								
1	0	.795	2.650	.265	2.11	2.04	2.12	2.04
1	0	1.325	"	"	2.36	2.11	2.14	2.09
1	0	1.855	"	"	2.74	2.25	2.48	2.21
1	0	2.250	"	"	4.00	2.49	3.91	2.37
1	0	.795	"	.106	2.06	2.05	2.03	2.03
1	0	1.325	"	"	2.14	2.10	2.10	2.09
1	0	1.855	"	"	2.32	2.18	2.24	2.21
1	0	2.250	"	"	2.61	2.33	2.59	2.40
6	.550	1.07	"	.1325	2.87	2.71	2.44	2.36
6	"	"	"	.265	2.80	2.48	2.51	2.42
6	"	"	"	.3975	2.60	2.34	2.63	2.66
10	"	"	"	.06625	2.30	2.27	2.45	2.36
10	"	"	"	.1325	2.31	2.22	2.35	2.14
10	"	"	"	.199	2.31	2.14	2.35	2.11

COMPARISON OF EXPERIMENTAL AND THEORETICAL RESULTS

FIGURE 11

IX CONCLUSIONS

Upon completion of the work a few comments and recommendations are in order concerning the method of approach and the results.

It must be remembered that the theoretical approximation is not exact and though the results of many authors were checked with the final equation, cases may exist where the approximation is in great error. This is most likely to happen for two types of disks. First, when the noncentral holes are near a boundary an additional stress concentration is supplied in appendix B. However, this effect was added after the bulk of the work was completed and its accuracy may only be implied since it gave satisfactory answers when applied to solved problems. No experimental results could be found with which to check with holes very near a boundary. Secondly, errors in the approximation may appear when there are many large holes in the disk (when L, the number of diameters center to center, is small). Here a shielding effect appears which reduces the stress on the inside edge of the noncentral hole. Stresses increase in the material between holes and may become larger than at either point 1 or point 2 which were investigated herein. Using evidence from experimental work, the stresses between the holes begins to predominate when L is less than 1.7.

Results obtained experimentally were satisfactory though certainly less experimental error would be desirable. Much of the laboratory

time was spent developing a method of obtaining results. Once a satisfactory approach was located, it was pursued until its validity was established. Better results could be achieved with a refinement in the equipment used, but the technique would remain basically the same. It is believed that the learning process would benefit little from such a continuation and it would be only time consuming and tedious. The method of high speed photography is recommended for future investigators as once the equipment is assembled, tests may be run quickly and easily. Its disadvantage is of course that the stressed disk is not available for static study. Such methods as Tardy compensation and locating isoclinics could then not be used.

X BIBLIOGRAPHY

1. S. Timoshenko and J. N. Goodier: Theory of Elasticity. McGraw-Hill Book Co., Inc., Second Edition, 1951.

2. T. Udoguchi: "Analysis of Centrifugal Stresses in a Rotating Disc Containing an Eccentric Circular Hole." The Japan Science Review, Series I, Vol. I., No. 1, 1949, pp. 53-63.

3. K. E. Barnhart, Jr., A. L. Hale, and J. L. Meriam: "Stresses in Rotating Disks Due to Noncentral Holes." Proceedings of the Society for Experimental Stress Analysis, Vol. IX, No. 1, 1951, pp 35-52.

4. R. E. Newton: "A Photoelastic Study of Stresses in Rotating Disks." A SME Transactions, Vol. 62, 1940, pp A-57 to A-62.

5. H. G. Edmunds: "Stress Concentrations at Holes in Rotating Discs." The Engineer, Vol. 198, No. 5154, Nov. 5, 1954, pp. 618-620.

6. Ta-Cheng Ku: "Stress Concentrations in a Rotating Disk with a Central Hole and Two Additional Symmetrically Located Holes." Transactions of the ASME, Vol. 27, Series E, No. 2, June, 1960, pp. 359-360.

7. Teverosky: Sov. Kotloburbo, No. 11, Nov., 1940.

8. E. K. Lynn: "Experimental Stress Analysis in the Design of a Liquid-hydrogen Pump Rotor." Experimental Mechanics, Vol. 2, No. 12, Dec., 1962, pp. 19A-23A.

9. P. P. Radkowski: "Stress in a Plate Containing a Ring of Circular Holes and a Central Circular Hole." Proceedings of the Second U. S. National Congress of Applied Mechanics, June, 1954, ASME, 1955, pp. 277-282.

10. R. C. J. Howland: "Stresses in a Perforated Strip." Proceedings of the Royal Society (London), Series A, Vol. 232, 1934, pp. 155-222.

11. K. J. Schulz: "On the State of Stress in Perforated Strips and Plates." Proceedings Nederland Akademie Van Wetenschappen, Vol. XLV, No. 3, 1940, pp. 233-239.

12. Chih-Bing Ling: "On the Stress in a Plate Containing Two Circular Holes." Journal of Applied Physics, Vol. 19, No. 1, Jan., 1948, pp. 77-82.

13. Z. Tuzi: "The Effect of a Circular Hole on the Stress Distribution in a Beam." Philosophical Magazine, Vol. 9, 1930.

14. M. Hetenyi: "The Application of Hardening Resins in the Three-Dimensional Photoelastic Studies." Journal of Applied Physics, Vol. 10, 1939, pp. 295-300.

15. R. D. Mindlin: "Stress Distribution Around a Hole Near the Edge of a Plate Under Tension." Proceedings of the Society for Experimental Stress Analysis, Vol. 5, No. 2, 1948, pp. 56-68.

16. M. M. Frocht: Photoelasticity. Vol. 1 and 2, John Wiley and Sons, Inc., New York, 1960.

17. J. J. Baruch: "The Design of a High-speed Polariscope", Proceedings of the Society for Experimental Stress Analysis, Vol. 8, No. 1, 1951.

18. W. A. Green, G. T. J. Hooper, and R. Hetherington: "Stress Distribution in Rotating Disks with Non-Central Holes", Aeronautical Quarterly, Vol. 15, pt. 2, May 1964, pp. 107-121.

19. Hysol Corporation, Olean, New York, Technical Data E-104D, "Photoelastic Cast Products, Hysol CP 5-4290," 1964.

20. Cadillac Plastic and Chemical Company, 15111 Second Avenue, Detroit 3, Michigan, Lexan brochure CDC 409 8-62, 1962.

21. K. Leist and J. Weber: "Optical Stress Distributions in Rotating Discs with Eccentric Holes," Report No. 57, Institute for Jet Propulsion: German Research Insitute for Aeronautics, Aachen, 1956.

22. A. San Miguel and E. N. Duran: "Some Low-modulus Birefringent Resins," Experimental Mechanics, Vol. 4, No. 3, March, 1964. pp. 84-88.

23. Katsuhiko Ito: "New Model Materials for Photoelasticity and Photoplasticity," Experimental Mechanics, Vol. 2, No. 12, Dec., 1962, pp. 373-376.

The vita has been removed from the scanned document

LIST OF SYMBOLS FOR APPENDIX

a	Poles on the x-axis of bipolar coordinates
b	Radius of hole
J	The quantity a $(\cosh E - \cos B)^{-1}$
K	A parametric coefficient
n	A positive integer, 0, 1, 2, 3, $\cdots$
T	Uniform tension on the edge of the plate
x	Longitudmal coordinate
y	Transverse coordinate
A	Value of E at the edge of the holes
θ	Angle measured from x-axis toward y-axis
Lb	Distance between centers of holes
E, B	Bipolar coordinates
S_{EE}	Tensile stress in the E direction
S_{BB}	Tensile stress in the B direction
S_{BE}	Shearing stress
χ	Stress function

XII APPENDIX A

An outline of the paper "On the Stress in a Plate Containing Two Circular Holes," by Chih-Bing Ling (reference 6).

For a theoretical solution to a plate containing two circular holes of equal size, two loading cases are discussed: one, a plate under uniform longitudinal tension T; and, two, a plate under uniform transverse tension T. See figure (1).

We must make use of bipolar coordinates (B,E) defined by

$$x + iy = -a \coth \frac{i}{2}(B + iE) \tag{1a}$$

where the two poles of the coordinates are located on the x-axis at the points (±a,o). Finding x and y independently, we get

$$x = J \sinh E \quad \text{and} \quad y = J \sin B \tag{2a}$$

$$\text{where} \quad \frac{a}{J} = \cosh E - \cos B. \tag{3a}$$

The biharmonic equation $\nabla^4 \chi = 0$, which must be satisfied by the stress function χ, then transforms to

$$\left(\frac{\partial^4}{\partial B^4} + 2\frac{\partial^4}{\partial B^2 \partial E^2} + \frac{\partial^4}{\partial E^4} + 2\frac{\partial^2}{\partial B^2} - 2\frac{\partial^2}{\partial E^2} + 1 \right) \frac{\chi}{J} = 0. \tag{4a}$$

Consider a solution, even in both B and E of the type

$$\frac{\chi}{J} = \Phi_n(E) \cos nB \tag{5a}$$

The transformed biharmonic equation then becomes, by substitution,

$$\left[\frac{d^4}{dE^4} - 2(n^2+1)\frac{d^2}{dE^2} + (n^2-1)\right]\phi_n(E) = 0. \tag{6a}$$

The solution even in E is

$$\phi_n(E) = A_n \cosh(n+1)E + B_n \cosh(n-1)E. \tag{7a}$$

For a solution which will give singularites at the poles, $x=\pm a$, a term must be added to equation (5a) so that

$$\frac{\chi_1}{J} = K(\cosh E - \cos B)\ln(\cosh E - \cos B) + \sum_{n=1}^{\infty} \phi_n(E)\cos nB \tag{8a}$$

where K is a parametric coefficient. The stresses derived from χ_1 are

$$a S_{EE} = \left[(\cosh E - \cos B)\frac{\partial^2}{\partial B^2} - \sinh E\frac{\partial}{\partial E} - \sin B\frac{\partial}{\partial B} + \cosh E\right]\frac{\chi_1}{J} \tag{9a}$$

$$a S_{BB} = \left[(\cosh E - \cos B)\frac{\partial^2}{\partial E^2} - \sinh E\frac{\partial}{\partial E} - \sin B\frac{\partial}{\partial B} + \cos B\right]\frac{\chi_1}{J} \tag{10a}$$

$$a S_{BE} = -(\cosh E - \cos B)\frac{\partial^2}{\partial B \partial E}\left(\frac{\chi_1}{J}\right). \tag{11a}$$

Examining $\frac{\chi_1}{J}$ we see that all of the stresses vanish at infinity,

provided that $\frac{\chi_1}{J} = 0$ when B, E = 0. This condition leads to

$$\sum_{n=1}^{\infty} (A_n + B_n) = 0. \tag{12a}$$

When the holes are absent from the infinite plate, the stress system will be specified by a symmetric stress function χ_o. When that two holes are present we use the stress function,

$$\chi = \chi_o + aT\chi_1 \tag{13a}$$

where aT is a factor introduced to make the coefficients in χ_1 dimensionless. These coefficients will then be adjusted to satisfy the boundary conditions at the edges of the holes.

Let the normal and tangential stress derived from χ_o at E=±A (edges of the holes) be

$$S_{EE} = T\sum_{n=0}^{\infty} c_n \cos nB \quad , \quad S_{BE} = T\sum_{n=0}^{\infty} b_n \sin nB \tag{14a}$$

Consequently, the boundary condition at E=±A is $S_{EE} = S_{BE} = 0$ which leads to $-2C_o = 2\phi_1(A) - K\cosh 2A$

for n=1, and for $n \geq 1$,

$$-2n = Q_{n-1} - 2Q_n \cosh A + Q_{n+1} - 2Q_n' \sinh A + 2K(\delta_{1n}\cosh A - \delta_{2n}) \tag{15a}$$

$$2b_n = Q'_{n-1} - 2Q'_n \cosh A + Q'_{n+1} + 2K\delta_{1n} \sinh A \qquad (15a)$$

where δ_{mn} is the Kronecher delta, the primes indicate differentiation, K is a coefficient to be determined, and

$$Q_n = (n-1)n(n+1)\,\phi_n(A) \quad , \quad Q'_n = n\phi'_n(A). \qquad (16a)$$

Simplifying equations (15a) we can express A_n and B_n explicitly in terms of C_n, b_n, and K. An addition equation (12a) is supplied for the determination of K. The problem is thus solved for any uniform stress state acting on the plate.

Two stress systems will be considered, (1) the plate under longitudinal tension T

$$\chi_o = \tfrac{1}{2} T y^2 \qquad (17a)$$

or $$\frac{\chi_o}{aTJ} = \frac{1}{2} \frac{\sin^2 B}{\cosh E - \cos B}$$

and, (2), the plate under transverse tension T

$$\chi_o = \tfrac{1}{2} T x^2$$

or, $$\frac{\chi_o}{aTJ} = \frac{1}{2} \frac{\sinh^2 E}{\cosh E - \cos B} \qquad (18a)$$

The stresses at $E=\pm A$ derived from χ_o are then

$$\left.\begin{aligned} (1)\ \frac{S_{EE}}{T}\Big|_A &= \left(\frac{1-\cosh A \cos B}{\cosh A - \cos B}\right)^2 \\ \frac{S_{BB}}{T}\Big|_A &= \left(\frac{\sinh A \sin B}{\cosh A - \cos B}\right)^2 \\ \frac{S_{BE}}{T}\Big|_A &= -\frac{\sinh A \sin B (1-\cosh A \cos B)}{(\cosh A - \cos B)^2} \end{aligned}\right\} \qquad (19a)$$

and (2)

$$\left.\begin{aligned} \frac{S_{EE}}{T}\Big|_A &= \left(\frac{\sinh A \sin B}{\cosh A - \cos B}\right)^2 \\ \frac{S_{BB}}{T}\Big|_A &= \left(\frac{1-\cosh A \cos B}{\cosh A - \cos B}\right) \\ \frac{S_{BE}}{T}\Big|_A &= \frac{\sinh A \sin B (1-\cosh A \cos B)}{(\cosh A - \cos B)^2} \end{aligned}\right\} \qquad (20a)$$

In the cases, by expanding the first and third expressions in a Fourier series between $B=-\pi$ and $B=\pi$, the coefficients c_o, c_n, and b_n may be evaluated. We thus have $\phi_1(A)$, Q_n, and Q'_n. A_n, B_n, and K may then be determined. In terms with an ambiguous sign, the upper sign goes with the longitudinal tension case (1) and the lower sign with the transverse tension case (2). K will be determined from

$$K\left[\frac{1}{2}+\tanh A\sinh^2 A-4\sum_{n=2}^{\infty}\frac{e^{-nA}\sinh n+n\sinh A(n\sinh A+\cosh A)}{n(n^2-1)(\sinh 2nA+n\sinh 2A)}\right] \tag{21a}$$

$$=\frac{1}{2}\pm\frac{1}{2}\mp 2\sinh^2 A\sum_{n=1}^{\infty}\frac{n}{\sinh 2nA+n\sinh 2A}\,.$$

For convenience, E and θ as shown in figure (1) will be related to B and A by

$$\cosh A=L\,,\quad \cos B=\frac{1+L\cos\theta}{L+\cos\theta}\,. \tag{22a}$$

The stress at the edges of the holes is found to be

$$\frac{S_{BB}}{T}=2(\cosh A-\cos B)\left[K\sinh A\left(1+4\sum_{n=1}^{\infty}\frac{\sinh nA\cos nB}{\sinh 2nA+n\sinh 2A}\right)\right.$$

$$\left.\mp 2\sum_{n=1}^{\infty}\frac{n(n\sinh nA\sinh A-\cosh nA\cosh A)\cos nB}{\sinh 2nA+n\sinh 2A}\right]. \tag{23a}$$

It appears that there are two points of maximum tensile stress at the edge of each hole. In the longitudinal tension case, these points are very nearly at $\theta = \pm \pi/2$, or, more precisely at $|\theta|$ slightly less than $\pi/2$. They shift toward $\theta = \pm\pi/2$ as L increases. For simplicity, the stress at $\theta = \pm\pi/2$ will be taken as the maximum with little error.

The limiting case $A = \infty$ (or $L = \infty$) corresponds to a single hole in the plate. In the limiting case where A=0 (L=1) the two holes touch.

XIII APPENDIX B

Results of the paper, "Stress Distribution around a Hole Near the Edge of a Plate Under Tension," by Raymond D. Mindlin (reference 15).

When the noncentral holes are near a boundary of the disk an additional stress concentration factor must be employed. The results found previously are to be multiplied by the factor found on the accompanying chart divided by three. That is, if the ratio C/R is 2.5, for the point near the boundary, pt. A, multiply by 3.4/3.0 and for the point on the hole most distant from the boundary, pt. B., multiply by 3.175/3.0. This will conveniently correct for the effect of a near edge of the disk.

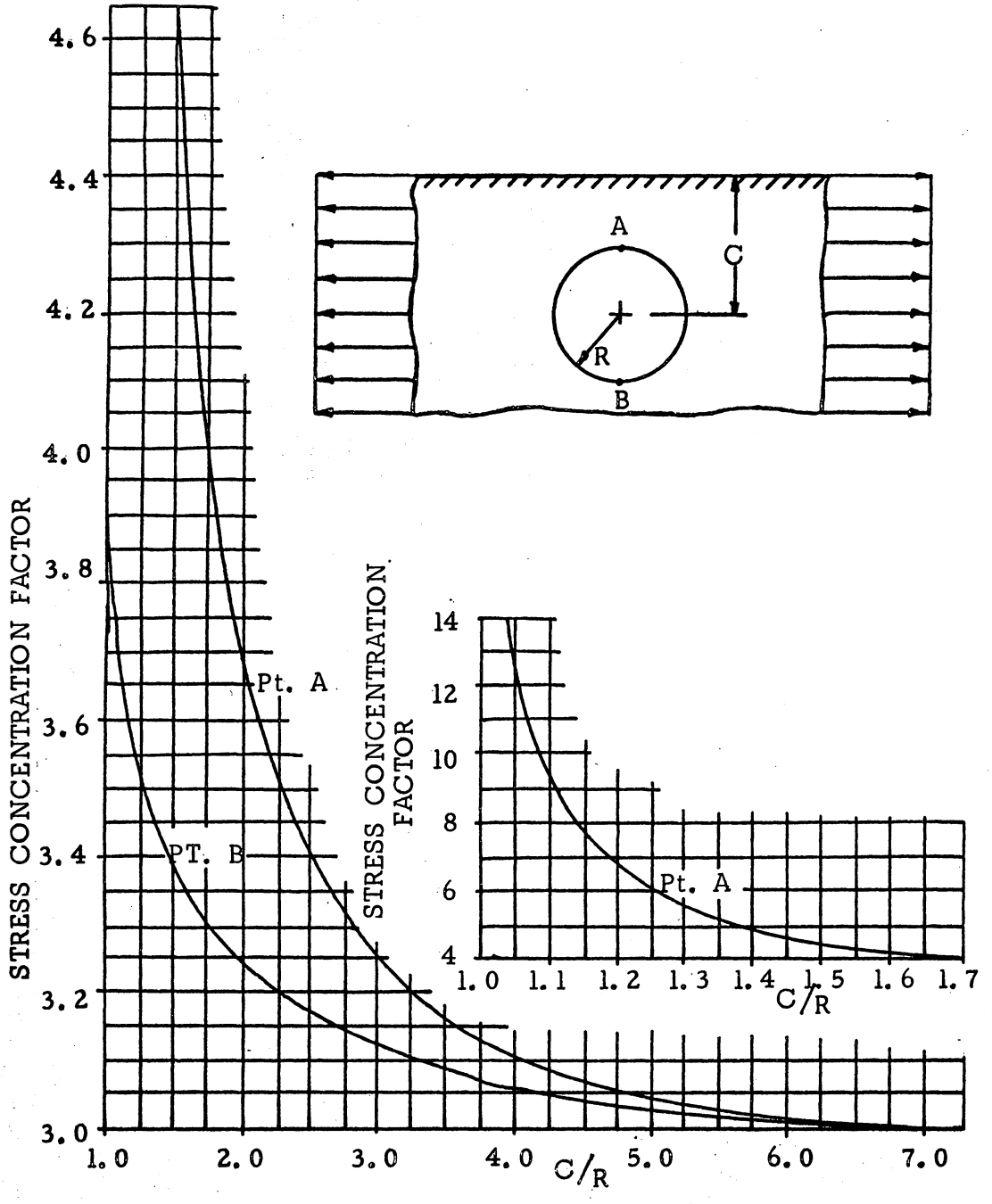

STRESS CONCENTRATIONS FOR A HOLE NEAR A BOUNDARY

FIGURE 12

ABSTRACT

The problem of finding the stress distribution about circular, noncentral holes in a spinning disk is discussed. A theoretical approximation is first developed using the methods of elasticity and combining solutions to similar problems from Ling (reference 6) and Timoshenko and Goodier (reference 2). Results are then found in the form of a maximum stress concentration factor which occurs at the edges of the holes. The accuracy of the derived solution is checked by obtaining values photoelastically from a similar spinning disk. Stress patterns are studied in photographs obtained with a strobe-flash and camera. The results are presented in a useable form for application to design.